Nonlinear Analysis: Hybrid Systems 61 (2026) 101754

Contents lists available at ScienceDirect

Nonlinear Analysis: Hybrid Systems

journal homepage: www.elsevier.com/locate/nahs

The link between equitable partitions and local agreements in multi-agent systems with nonlinear interactions☆,☆☆

Anthony Couthures [a,*], Vineeth Satheeskumar Varma [a,b], Samson Lasaulce [a], Irinel-Constantin Morărescu [a,b]

[a] Université de Lorraine, CNRS, CRAN, Nancy, F-54000, France
[b] Automation Department, Technical University of Cluj-Napoca, Cluj-Napoca, Romania

ARTICLE INFO

Keywords:
Multi-agent systems
Nonlinear interactions
Equitable partitions

ABSTRACT

Classically, global consensus is achieved in linear multi-agent systems that interact over a connected, unsigned graph. However, when the interactions are non-linear, agents may get polarized, i.e., they synchronize locally within communities while the communities do not reach a consensus with each other. In this context, we demonstrate that local synchronizations strongly rely on the existence of equitable partitions in the graph. Specifically, if some agents synchronize independently of the initial conditions, we prove that these agents must belong to the same cell of an equitable partition. On top of that, based on forward invariance properties, we are able to characterize the stability of local synchronization equilibria in terms of the stability of equilibria of a quotient graph defined by an equitable partition.

1. Introduction

The research on consensus in multi-agent systems is very extensive. Researchers have established conditions for achieving consensus in various scenarios, including systems with continuous or discrete-time dynamics, directed or undirected interactions, and fixed or time-varying interaction weights [1–3]. Most of the existing studies consider that agents update their state using feedback from the neighbors' state in the interaction graph. In this setup, these works highlight that network connectivity is crucial to reach consensus. Indeed, polarization or local synchronization is traditionally obtained by either removing network connectivity by cutting links in the interaction graph [4,5], or allowing antagonistic interactions [6,7].

It should be noted that global synchronization in large networks is a rather rare phenomenon. Thus, there is an increasing need for the development of models and tools allowing us to understand the behavior of complex networks in social sciences, economics, biology, and engineering. Clustering and community detection have received a lot of attention during the past decades [8]. The most common formulations of this problem in the literature involve the optimization of the modularity function [9] or partition stability [10].

This paper follows the path opened by [11–13] by assuming that agents update their states based on some nonlinear perception, or signal, of the neighbors' states. In this case, although we assume a continuous-time multi-agent dynamics with *fixed, undirected interactions defining a connected graph, one may reach local agreements in clusters*. Specifically, the dynamics of each agent is driven by the difference between its current state and a normalized sum of signals received from its neighbors, where these signals are

☆ This article is part of a Special issue entitled: 'TC 1.5 Networked systems (IFAC WC 2026)' published in Nonlinear Analysis: Hybrid Systems.
☆☆ This work was funded by the CNRS MITI project BLESS.
* Corresponding author.
E-mail address: anthony.couthures@univ-lorraine.fr (A. Couthures).

https://doi.org/10.1016/j.nahs.2026.101754
Received 23 October 2025; Received in revised form 23 February 2026; Accepted 16 May 2026

generated by applying a common nonlinear function, denoted by s, to the neighbors' states. We note that similar models have been considered by [14], where the sum of the signals is replaced by the signal of the sum, by [15], where the stability of the origin is analyzed when the interaction is based on individual signals from neighbors, and correspond exactly to [16] for sigmoidal interaction function.

The study of clustered behavior in networked systems has traditionally focused on how network symmetries, specifically equitable partitions, drive synchronization patterns in systems with linear diffusive coupling [17–19]. Moreover, the equitable partitions are explicitly linked to the controllability of robot swarms and how leaders influence clusters [20,21]. It is also noteworthy that empirical studies have already emphasized the ability of quotient graphs (induced by equitable partitions) to reproduce the asymptotic behavior of a large graph [22].

However, many real-world challenges involve agents subject to nonlinear input constraints or perception filters, a gap partially explored in the context of antagonistic interactions [14]. Addressing scenarios with cooperative but nonlinear interactions is essential for practical implementation in two key domains. First, in *engineering and robotics*, the nonlinear function s serves as a proxy for sensor saturation, quantization, or limited communication bandwidth [23]. Our results demonstrate how the interaction topology can maintain stable sub-formations (clusters) explicitly through the network topology, even when individual actuation is saturated. Second, in *social opinion dynamics*, s models confirmation bias and amplification phenomena [11,12]. Unlike standard models that require cutting links or introducing antagonism to explain polarization, our framework reveals how "echo chambers" (local exact agreements) can persist as stable equilibria on connected, purely cooperative graphs due to structural symmetries in the social network.

To formalize these phenomena, this paper establishes a fundamental link between the topological structure of the interaction graph and the emergence of these local agreement equilibria. While previous works have utilized graph partitions for linear interactions or specific bifurcations [14,24], we prove that for a general class of nonlinear perception functions, the existence of exact local agreements is structurally determined by the presence of a weight-regular partition. We further focus on the stricter condition of *equitable partitions*, which ensures not only the existence of equilibria but also the forward invariance of the cell-synchronized manifold. By exploiting this invariance, we perform an exact model reduction, collapsing the high-dimensional network dynamics into a tractable quotient system. This reduction allows us to derive a sufficient condition for exponential stability by decoupling the analysis into quotient dynamics (cluster trajectories) and transversal dynamics (internal cohesion).

The rest of the manuscript is organized as follows. Section 2 introduces the instrumental concepts and tools required for our analysis. Section 3 establishes the structural requirement for clustered equilibria, demonstrating that they are supported by equitable partitions of the network graph. In Section 4, we show that the dynamics respect this structure by proving the forward invariance of the cell-synchronized manifold and deriving the lower-dimensional quotient dynamics of the cell states. Section 5 is dedicated to the analysis of this quotient system. Finally, Section 6 provides conditions for the local exponential stability of a clustered equilibrium. Some conclusions and perspectives end the presentation.

Notation $\mathbb{R}$ denotes the set of real numbers. If $\boldsymbol{x} \in \mathbb{R}^N$, then x_i is the ith component of $\boldsymbol{x}$ and define $\boldsymbol{x}_{-i} = (x_1, \dots, x_{i-1}, x_{i+1}, \dots, x_N) \in \mathbb{R}^{N-1}$ the vector of all components of $\boldsymbol{x}$ except the ith one. For a matrix $\boldsymbol{A} \in \mathbb{R}^{N\times N}$, we denote by a_{ij} the element of $\boldsymbol{A}$ in the ith row and jth column. We denote by $\mathbf{1}_N \in \mathbb{R}^N$ the vector with all components equal to 1 and for a set $\mathcal{M} \subset \{1, \dots, N\}$, we denote by $\mathbb{1}_{\mathcal{M}} \in \mathbb{R}^N$ the column vector such that $[\mathbf{1}_{\mathcal{M}}]_k = 1$ if $k \in \mathcal{M}$ and 0 otherwise. For $\boldsymbol{x} \in \mathbb{R}^N$, we denote by $\|\boldsymbol{x}\| = (\boldsymbol{x}^\top \boldsymbol{x})^{\frac{1}{2}}$ the Euclidean norm of $\boldsymbol{x}$. Moreover, we denote by $\mathrm{diag}(\boldsymbol{x}) \in \mathbb{R}^{N\times N}$ the diagonal matrix with the vector $\boldsymbol{x} \in \mathbb{R}^N$ on the diagonal.

2. Preliminaries

2.1. Graph structure and network interaction

We consider a set $\mathcal{V} = \{1, \dots, N\}$ of N agents whose interactions are described by the graph $\mathcal{G} = (\mathcal{V}, \mathcal{E})$ where $\mathcal{E} \subset \mathcal{V} \times \mathcal{V}$. We denote by $\boldsymbol{A} = (a_{ij})_{i,j\in\mathcal{V}} \in \mathbb{R}^{N\times N}$ the *adjacency matrix* of $\mathcal{G}$. Thus $a_{ij} = 1$ if there is an edge between $i \in \mathcal{V}$ and $j \in \mathcal{V}$ (i.e., $(i, j) \in \mathcal{E}$), and $a_{ij} = 0$ otherwise. The *degree matrix* $\boldsymbol{D} \in \mathbb{R}^{N\times N}$ is a diagonal matrix with diagonal elements $d_i = \sum_{j=1}^{N} a_{ij}$, representing the degree of each vertex i. S

The *neighborhood* of agent i is $\mathcal{N}_i := \{j \in \mathcal{V} \mid (j, i) \in \mathcal{E}\}$. The cardinality of $\mathcal{N}_i$ is the degree d_i. A *path* in $\mathcal{G}$ is a sequence of edges $(i_1, i_2), (i_2, i_3), \dots, (i_p, i_{p+1})$ where $(i_k, i_{k+1}) \in \mathcal{E}$ for all $k \in \{1, \dots, p\}$. Two vertices $i, j \in \mathcal{V}$ are *connected* if there exists a path in $\mathcal{G}$ connecting them. The graph $\mathcal{G}$ is *connected* if every pair of vertices is connected through a path.

Assumption 1. The graph $\mathcal{G} = (\mathcal{V}, \mathcal{E})$ is fixed, undirected, and connected.

2.2. Signal function and communication model

To each agent i we assign a scalar normalized state value $x_i \in [-1, 1]$. Agents interact and update their states based on signals received from their neighbors. The interaction process is modeled through a **common signal function** $s : [-1, 1] \to [-1, 1]$, assumed to be **non-decreasing** and **Lipschitz-continuous**. The formulation is quite general; it encompasses the standard linear consensus model when $s(x) = x$, but also accommodates a wide range of nonlinearities including saturation effects (e.g., sigmoidal functions like $\tanh$) [14,25], potential biases (affine functions), and continuous approximations of discontinuous phenomena like quantization [11,12].

2.3. Agent and collective dynamics

The state of each agent i evolves according to the following dynamics:

$$\dot{x}_i = \frac{1}{d_i}\sum_{j=1}^{N} a_{ij} s(x_j) - x_i. \tag{1}$$

The collective dynamics of all agents can be expressed in vector form as:

$$\dot{\boldsymbol{x}} = \boldsymbol{D}^{-1}\boldsymbol{A}\boldsymbol{s}(\boldsymbol{x}) - \boldsymbol{x} := \boldsymbol{f}(\boldsymbol{x}), \tag{2}$$

where $\boldsymbol{x} = (x_1, \dots, x_N)^\top \in \mathcal{X} := [-1,1]^N$ is the vector of agent states and $\boldsymbol{s}(\boldsymbol{x}) = (s(x_1), \dots, s(x_N))^\top$.

The state space described by the hypercube $\mathcal{X}$ is forward invariant [13, Proposition 1], ensuring that solutions remain bounded.

Remark 1 (*Normalization and Physical Constraints*)**.** The choice of the compact state space $\mathcal{X} = [-1,1]^N$ is motivated by both phenomenological and theoretical considerations. From a modeling perspective, this constraint captures inherent physical limitations, such as actuator saturation in engineering systems or the bounded nature of opinions (e.g., spanning from extreme disagreement to agreement) in social dynamics [11,16]. Theoretically, $[-1,1]^N$ serves as a canonical form for systems driven by bounded signal functions. Consider a general signal function $s : \mathbb{R} \to \mathbb{R}$ with extremal fixed points $\underline{c} = \min\{c \in \mathbb{R} \mid s(c) = c\}$ and $\overline{c} = \max\{c \in \mathbb{R} \mid s(c) = c\}$. As a direct consequence of the proof of [26, Proposition 1], the hypercube $[\underline{c}, \overline{c}]^N$ is forward invariant and attractive for the dynamics (2). Since the analysis on any hypercube $[\underline{c}, \overline{c}]^N$ is equivalent to that on $[-1,1]^N$ via an affine transformation, our formulation introduces no loss of generality. This assumption ensures the vector field is uniformly bounded, allowing our analysis to focus on the structural relationship between network topology and emergent cluster equilibria.

2.4. Clustered equilibria

As shown in [13], the nonlinear interactions defined by s lead to complex and structured equilibria that may be different from the global agreement. We are particularly interested in states of *local agreement*, where the agents self-organize into distinct, internally synchronized clusters.

Definition 1 (*Partition*)**.** A *partition* of the set $\mathcal{V}$ is a collection of non-empty subsets $\pi = \{C_1, \dots, C_M\}$, called *cells*, such that $\bigcup_{k=1}^{M} C_k = \mathcal{V}$ and $C_k \cap C_l = \emptyset$ for all $k \neq l$. We denote the number of agents in cell C_k as its cardinality, $N_k = |C_k|$.

The structured states that we study are described below.

Definition 2 (*Cell Synchronized State*)**.** A state vector $\boldsymbol{x} \in \mathcal{X}$ is said to be *Cell Synchronized (CS)* with respect to a partition π if for every cell $C_k \in \pi$, all agents within the cell have the same state value: $x_i = x_j, \forall i, j \in C_k$.

This allows us to define the following notion of equilibrium.

Definition 3 (*Cell Synchronized Equilibrium*)**.** An equilibrium $\boldsymbol{x}^* \in \mathcal{X}$ of (2) is said to be a *Cell Synchronized Equilibrium (CSE)* if it is a CS vector for a partition π.

The central questions of our work are: Which structural properties must a graph $\mathcal{G}$ and a partition π possess to guarantee that a *Cell Synchronized Equilibrium (CSE)* can exist for a general class of signals s? How can we characterize the stability of the CSEs?

3. The structural implications of CSE

Let us consider a partition $\pi = \{C_1, \dots, C_M\}$ of the vertex set $\mathcal{V}$. Our objective is to find conditions under which the system (2) can have a CSE $\boldsymbol{x}^*$ with respect to π. Such an equilibrium is characterized by the existence of $\boldsymbol{y}^* = (y_1^*, \dots, y_M^*)^\top \in \mathcal{Y} := [-1,1]^M$ such that for any agent $i \in C_k$ one has $x_i^* = y_k^*$.

At the equilibrium one has $\dot{x}_i = 0, \ \forall i \in \mathcal{V}$, which yields:

$$x_i^* = \frac{1}{d_i}\sum_{j \in \mathcal{N}_i} s(x_j^*). \tag{3}$$

Let us apply the cell-synchronized assumption to this equation for an arbitrary agent $i \in C_k$. The left-hand side becomes $x_i^* = y_k^*$. The sum on the right-hand side can be reorganized by grouping the neighbors of i according to the cells to which they belong. Let $b_{il} := |\mathcal{N}_i \cap C_l|$ be the number of neighbors of agent i in cell C_l. The equilibrium condition for agent $i \in C_k$ can thus be written as:

$$y_k^* = \frac{1}{d_i}\sum_{l=1}^{M} b_{il} s(y_l^*). \tag{4}$$

Since (3) holds for *every* agent within the cell C_k, taking $i' \in C_k$ (where $i' \neq i$), its equilibrium state must also be y_k^*, leading to:

$$y_k^* = \frac{1}{d_{i'}}\sum_{l=1}^{M} b_{i'l} s(y_l^*). \tag{5}$$

Eqs. (4) and (5) are simultaneously satisfied for any arbitrary vector of cell values $\boldsymbol{y}^*$ (and thus for any signal s), if the following identity hold:

$$\sum_{l=1}^{M} \left(\frac{b_{il}}{d_i} - \frac{b_{i'l}}{d_{i'}} \right) s(y_l^*) = 0, \quad \forall \boldsymbol{y}^* \in \mathcal{Y}.$$

This linear combination of the functions $s(y_l^*)$ is identically zero for any non-trivial choice of s, if all the coefficients are zero. This gives us the necessary condition:

$$\frac{b_{il}}{d_i} = \frac{b_{i'l}}{d_{i'}}, \quad \forall l \in \{1, \dots, M\} \text{ and } \forall i, i' \in C_k. \tag{6}$$

This condition defines a *weight regular partition*. However, our goal is to link the dynamics to the purely combinatorial and structural properties of the graph. A stronger condition is to require the degree of neighbors in the cell to be constant. This condition, known as equitable partition, is standard in algebraic graph theory, as it ensures that the column space of the characteristic matrix $\boldsymbol{P}$ (defined below) is an invariant subspace of the adjacency matrix $\boldsymbol{A}$. We therefore adopt this stronger, more fundamental definition. As we prove next, the equitable partition condition implies that (6) is automatically satisfied.

3.1. Formalizing the structure: Equitable partitions (EP)

We now formalize the equitable partition and all the structural concepts needed for the subsequent analysis.

Definition 4 (*Equitable Partition (EP)*)**.** A partition $\pi = \{C_1, \dots, C_M\}$ of $\mathcal{V}$ is called *equitable* if for any two cells C_k and C_l, the number of neighbors in C_l of any vertex $i \in C_k$ is a constant b_{kl} that is independent of the choice of $i \in C_k$.

Remark 2 (*Constant Degree in Each Cell*)**.** Definition 4 implies that all vertices within the same cell C_k of an equitable partition must have the same degree, denoted d_{C_k}. It is therefore *weight regular* and verifies condition (6).

In the sequel, we introduce the tools to describe the EPs.

Definition 5 (*Characteristic Matrix*)**.** A partition π is represented by a *characteristic matrix* $\boldsymbol{P} \in \mathbb{R}^{N \times M}$ where $P_{ik} = 1$ if the vertex $i \in C_k$, and $P_{ik} = 0$ otherwise. The cell-synchronized state condition is then expressed as $\boldsymbol{x}^* = \boldsymbol{P}\boldsymbol{y}^*$.

Definition 6 (*Quotient and Induced Graphs*)**.** Given a graph $\mathcal{G}$ and an EP π:

- The *quotient graph* $\mathcal{G}/\pi$ describes the external connections between cells. It is a directed graph on M vertices with a weighted adjacency matrix $\boldsymbol{B} = (b_{kl}) \in \mathbb{R}^{M \times M}$.
- For each cell C_k, the *induced subgraph* $\mathcal{G}_k = (C_k, \mathcal{E}_k)$, where $\mathcal{E}_k = \mathcal{E} \cap (C_k \times C_k)$, describes the internal connections within the cell. Its topology is given by the *cell adjacency matrix* $\boldsymbol{A}_k$.

Moreover, an EP π is said to be *connected* if each induced subgraph $\mathcal{G}_k$ is connected.

Example 1. For the graph of Fig. 1 with the EP $\pi = \{C_1, \dots, C_5\}$, the characteristic matrix $\boldsymbol{P}$ and the adjacency matrix $\boldsymbol{B}$ of the quotient graph are given by

$$\boldsymbol{P}^\top = \begin{bmatrix} \mathbb{1}_{C_1} & \mathbb{1}_{C_2} & \mathbb{1}_{C_3} & \mathbb{1}_{C_4} & \mathbb{1}_{C_5} \end{bmatrix} \text{ and } \boldsymbol{B} = \begin{bmatrix} 2 & 2 & 0 & 0 & 0 \\ 3 & 1 & 1 & 0 & 0 \\ 0 & 2 & 0 & 1 & 0 \\ 0 & 0 & 1 & 0 & 3 \\ 0 & 0 & 0 & 1 & 2 \end{bmatrix},$$

where $\mathbb{1}_{C_i} \in \mathbb{R}^{10}$ (see the Notation section). Note that the adjacency matrix $\boldsymbol{B}$ is not symmetric and contains self-loops.

3.2. A foundational example: Twin node synchronization

The simplest non-trivial example of a cell in an EP consists of two "twin" nodes. This concept provides a link between local symmetry and local synchronization.

Definition 7 (*Twin Nodes*)**.** Two distinct agents $i, j \in \mathcal{V}$ are called *twins*, denoted $i \sim j$, if their neighborhoods, excluding each other, are identical: $\mathcal{N}_i \setminus \{j\} = \mathcal{N}_j \setminus \{i\}$.

If two nodes i and j are twins, then the partition containing the cell $C_k = \{i, j\}$ (with all other nodes in singleton cells) is equitable. This elementary symmetry has a direct dynamic consequence.

Proposition 1. *Let $i, j \in \mathcal{V}$ be twin agents. Then, under the dynamics (2), they asymptotically synchronize, i.e., $\lim_{t \to \infty}(x_i(t) - x_j(t)) = 0$. Moreover, the convergence is exponential.*

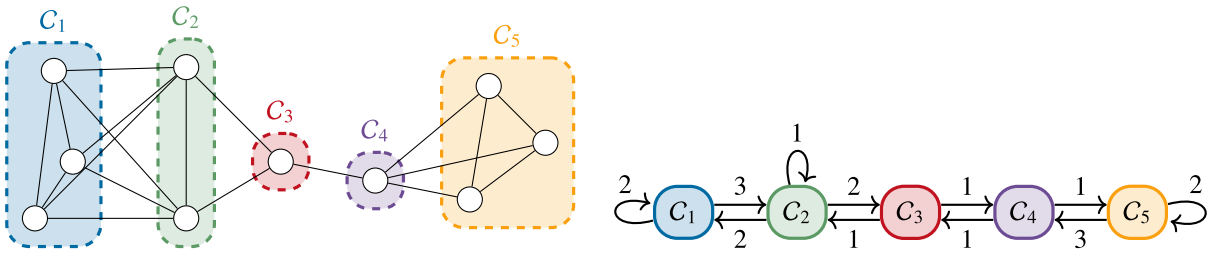

(a) A graph with a connected equitable partition. (b) Quotient graph of the graph (a) with the partition $\pi = \{C_1, \dots, C_5\}$.

Fig. 1. Example of a graph with equitable partition and its quotient graph.

Proof. Consider the difference $\delta_{ij} = x_i - x_j$. Since i and j are twins, they have the same degree $d_i = d_j$. The dynamics of the difference is given by

$$\begin{aligned}\dot{\delta}_{ij} &= \dot{x}_i - \dot{x}_j = \frac{1}{d_i}\sum_{k\in\mathcal{N}_i} s(x_k) - \frac{1}{d_j}\sum_{k\in\mathcal{N}_j} s(x_k) + x_j - x_i \\ &= \frac{1}{d_i}\Big[\sum_{k\in\mathcal{N}_i\setminus\{j\}} s(x_k) - \sum_{k\in\mathcal{N}_j\setminus\{i\}} s(x_k) - s(x_i) + s(x_j)\Big] - \delta_{ij} \\ &= \frac{1}{d_i}\left[s(x_j) - s(x_i)\right] - \delta_{ij}.\end{aligned}$$

Consider the Lyapunov function $V(\delta_{ij}) = \delta_{ij}^2/2$. Its time derivative is

$$\dot{V}(\delta_{ij}) = \delta_{ij}\dot{\delta}_{ij} = \delta_{ij}\left[\frac{1}{d_i}[s(x_j) - s(x_i)] - \delta_{ij}\right] = -\frac{1}{d_i}(x_i - x_j)(s(x_i) - s(x_j)) - \delta_{ij}^2.$$

Since s is non-decreasing, the term $(x_i - x_j)(s(x_i) - s(x_j)) \geq 0$. Therefore, $\dot{V}(\delta_{ij}) \leq -\delta_{ij}^2 = -2V(\delta_{ij})$, which guarantees exponential convergence of $\delta_{ij}(t)$ to zero. □

4. Dynamics on the equitable partition manifold

Having established that EP structure ensures the existence of CSE, we now demonstrate that the dynamics (2) preserve the CSE induced by this EP structure. This allows us to perform a model reduction, simplifying the N-dimensional system to a more tractable M-dimensional one that governs the evolution of the cell states.

4.1. Forward invariance of the cell-synchronized manifold

Definition 8. Given a graph $\mathcal{G}$ with an EP π, the *Cell Synchronized Manifold*, denoted $\mathcal{S}_\pi$, is the subspace of states that are cell-synchronized with respect to π:

$$\mathcal{S}_\pi = \{\boldsymbol{x} \in \mathcal{X} \mid \boldsymbol{x} = \boldsymbol{P}\boldsymbol{y} \text{ for some } \boldsymbol{y} \in \mathcal{Y}\}. \tag{7}$$

The following proposition confirms that, if the agents in each cell start synchronized, they will always remain synchronized.

Proposition 2. *Let π be an EP of the graph $\mathcal{G}$. The cell-synchronized manifold $\mathcal{S}_\pi$ is forward invariant with respect to the dynamics (2).*

Proof. Consider an initial state $\boldsymbol{x}(0) \in \mathcal{S}_\pi$. By definition, there exists a vector $\boldsymbol{y}(0) \in \mathcal{Y}$ such that $\boldsymbol{x}(0) = \boldsymbol{P}\boldsymbol{y}(0)$. This means that for any cell C_k, all agents $i \in C_k$ have the same initial state, $x_i(0) = y_k(0)$.

To prove invariance, we must show that the time derivatives $\dot{x}_i(t)$ are identical for all agents i within the same cell C_k at any time t where $\boldsymbol{x}(t) \in \mathcal{S}_\pi$. Let us examine the dynamics for an arbitrary agent $i \in C_k$:

$$\dot{x}_i(t) = \frac{1}{d_i}\sum_{j=1}^{N} a_{ij}\, s(x_j(t)) - x_i(t).$$

Since $\boldsymbol{x}(t) \in \mathcal{S}_\pi$, we can substitute $x_j(t) = y_l(t)$ for all $j \in C_l$, and $x_i(t) = y_k(t)$. We can group the sum over neighbors by the cells they belong to:

$$\sum_{j=1}^{N} a_{ij}\, s(x_j(t)) = \sum_{l=1}^{M}\sum_{j\in\mathcal{N}_i\cap C_l} s(y_l(t)) = \sum_{l=1}^{M} b_{kl}\, s(y_l(t)).$$

The last step follows from Definition 4, as the number of neighbors of $i \in C_k$ in cell C_l is the constant b_{kl}. As established in Section 3, the degree d_i is also constant for all $i \in C_k$, equal to d_{C_k}. Substituting these back, we get:

$$\dot{x}_i(t) = \frac{1}{d_{C_k}} \sum_{l=1}^{M} b_{kl} s(y_l(t)) - y_k(t).$$

This expression for $\dot{x}_i(t)$ depends only on the index of its cell, k, and not on the specific agent i. Therefore, for any two agents $i, i' \in C_k$, we have $\dot{x}_i(t) = \dot{x}_{i'}(t)$. Since they share the same initial state and the same derivative, their states will remain identical for all $t \geq 0$. This holds for all cells, so $\boldsymbol{x}(t)$ remains in S_π. □

4.2. Derivation of the quotient dynamics

Proposition 2 allows us to perform an exact model reduction. Since the dynamics on S_π preserves cell synchronization, we can derive a lower-dimensional model that describes the evolution of the cell values $\boldsymbol{y}$ directly.

To proceed, we first state a standard result from algebraic graph theory that formalizes the relationship between the full graph matrices $(\boldsymbol{A}, \boldsymbol{D})$ and the quotient/partition matrices $(\boldsymbol{B}, \boldsymbol{P})$.

Lemma 1. *Let π be an EP with characteristic matrix $\boldsymbol{P}$ and quotient matrix $\boldsymbol{B}$. Let $\tilde{\boldsymbol{D}} = \mathrm{diag}(d_{C_1}, \dots, d_{C_M})$ be the diagonal matrix of cell degrees. The following identities hold:*

(i) $\boldsymbol{A}\boldsymbol{P} = \boldsymbol{P}\boldsymbol{B}$,
(ii) $\boldsymbol{D}\boldsymbol{P} = \boldsymbol{P}\tilde{\boldsymbol{D}}$,
(iii) $\boldsymbol{D}^{-1}\boldsymbol{P} = \boldsymbol{P}\tilde{\boldsymbol{D}}^{-1}$.

Proof. (i) See [27, Lemma 9.3.1]. (ii) The (i,k)-th entry of $\boldsymbol{D}\boldsymbol{P}$ is $d_i P_{ik}$. If $i \notin C_k$, $P_{ik} = 0$. If $i \in C_k$, the entry is $d_i = d_{C_k}$. The (i,k)-th entry of $\boldsymbol{P}\tilde{\boldsymbol{D}}$ is $\sum_l P_{il}\tilde{D}_{lk} = P_{ik}\tilde{D}_{kk} = P_{ik}d_{C_k}$. This is also d_{C_k} if $i \in C_k$ and 0 otherwise. (iii) Follows directly from (ii) by multiplying it by the inverse matrices in both sides. □

We now derive the quotient dynamics.

Proposition 3. *For any state $\boldsymbol{x}(t) \in S_\pi$ with $\boldsymbol{x}(t) = \boldsymbol{P}\boldsymbol{y}(t)$, the dynamics of the cell values $\boldsymbol{y}(t)$ is governed by the following M-dimensional* ***quotient dynamics****:*

$$\dot{\boldsymbol{y}} = \tilde{\boldsymbol{D}}^{-1}\boldsymbol{B}\boldsymbol{s}(\boldsymbol{y}) - \boldsymbol{y}. \tag{8}$$

Proof. We start with the collective dynamics (2): $\dot{\boldsymbol{x}} = \boldsymbol{D}^{-1}\boldsymbol{A}\boldsymbol{s}(\boldsymbol{x}) - \boldsymbol{x}$. Since $\boldsymbol{x} = \boldsymbol{P}\boldsymbol{y}$, we have $\dot{\boldsymbol{x}} = \boldsymbol{P}\dot{\boldsymbol{y}}$. The signal function acts element-wise, so for any $i \in C_k$, we have $s(x_i) = s(y_k)$. This implies the vector relation $\boldsymbol{s}(\boldsymbol{x}) = \boldsymbol{s}(\boldsymbol{P}\boldsymbol{y}) = \boldsymbol{P}\boldsymbol{s}(\boldsymbol{y})$. Substituting these into the dynamics yields:

$$\boldsymbol{P}\dot{\boldsymbol{y}} = \boldsymbol{D}^{-1}\boldsymbol{A}(\boldsymbol{P}\boldsymbol{s}(\boldsymbol{y})) - \boldsymbol{P}\boldsymbol{y}.$$

Now we apply the identities from Lemma 1. First, we replace $\boldsymbol{A}\boldsymbol{P}$ with $\boldsymbol{P}\boldsymbol{B}$:

$$\boldsymbol{P}\dot{\boldsymbol{y}} = \boldsymbol{D}^{-1}\boldsymbol{P}\boldsymbol{B}\boldsymbol{s}(\boldsymbol{y}) - \boldsymbol{P}\boldsymbol{y}.$$

Next, we replace $\boldsymbol{D}^{-1}\boldsymbol{P}$ with $\boldsymbol{P}\tilde{\boldsymbol{D}}^{-1}$:

$$\boldsymbol{P}\dot{\boldsymbol{y}} = \boldsymbol{P}\tilde{\boldsymbol{D}}^{-1}\boldsymbol{B}\boldsymbol{s}(\boldsymbol{y}) - \boldsymbol{P}\boldsymbol{y} = \boldsymbol{P}\left(\tilde{\boldsymbol{D}}^{-1}\boldsymbol{B}\boldsymbol{s}(\boldsymbol{y}) - \boldsymbol{y}\right).$$

The columns of the characteristic matrix $\boldsymbol{P}$ are linearly independent. We can therefore left-multiply by the pseudo-inverse $\boldsymbol{P}^{\#} = (\boldsymbol{P}^\top\boldsymbol{P})^{-1}\boldsymbol{P}^\top$ to isolate $\dot{\boldsymbol{y}}$, which yields the quotient dynamics (8). □

Remark 3 (*Equilibrium Equivalence*)**.** Proposition 3 establishes an equivalence between the full dynamics (2) on the manifold S_π and the lower-dimensional quotient dynamics (8). A direct consequence is that a cell-synchronized state $\boldsymbol{x}^* = \boldsymbol{P}\boldsymbol{y}^*$ is an equilibrium of the full system (2) if and only if its corresponding cell-value vector $\boldsymbol{y}^*$ is an equilibrium of the quotient system (8). This simplifies the search for all possible CSEs in finding the equilibria of the more tractable M-dimensional system. However, it is important to note that the full system may possess other equilibria that are not cell-synchronized. Therefore, we cannot always describe the full system by this reduced model.

Remark 4 (*Extension to Directed Graphs*)**.** It is worth noting that the results in Sections 3 and 4 regarding the existence of CSEs and the derivation of the quotient dynamics do not strictly require the graph $\mathcal{G}$ to be undirected. In the context of directed graphs, Definition 4 corresponds to a *row-equitable partition*, where the out-degree of every node in cell C_k pointing to nodes in cell C_l is constant. Under this condition, the algebraic identity $\boldsymbol{A}\boldsymbol{P} = \boldsymbol{P}\boldsymbol{B}$ holds even for asymmetric adjacency matrices. Consequently, the forward invariance of S_π (Proposition 2) and the reduced quotient model (Proposition 3) remain valid for directed strongly connected graphs.

5. Analysis of the quotient system

The derivation of the quotient dynamics in Section 4 provides us with a useful analytical tool. The problem of finding CSEs on an N-dimensional system has been reduced to the problem of finding the equilibria of the M-dimensional system (8). In this section, we analyze this quotient system to first guarantee the existence of such equilibria, and then to characterize how their number and type depend on the relation between the network structure and the nonlinearity of the signal function.

5.1. Existence of local agreement equilibria

Our first step is to confirm that the quotient system is well-behaved and possesses at least one equilibrium point. This result directly implies the existence of at least one CSE in the original full-scale system.

Proposition 4. *The quotient dynamics (8) has at least one equilibrium point $\boldsymbol{y}^* \in \mathcal{Y}$.*

Proof. The function $\boldsymbol{g}(\boldsymbol{y}) = \tilde{\boldsymbol{D}}^{-1}\boldsymbol{B}\boldsymbol{s}(\boldsymbol{y})$ is continuous on the compact convex set $\mathcal{Y}$ since s is continuous. Furthermore, coordinates of $\boldsymbol{g}(\boldsymbol{y})$ are convex combinations of values $s(y_j) \in [-1, 1]$, thus $\boldsymbol{g}(\boldsymbol{y}) \in \mathcal{Y}$. By Brouwer's Fixed Point Theorem, $\boldsymbol{g}$ must have at least one fixed point $\boldsymbol{y}^* \in \mathcal{Y}$. □

5.2. Characterization and bifurcation of equilibria

Although its existence is guaranteed, the nonlinear nature of s may lead to the emergence of multiple CSE. To understand this phenomenon, we analyze the equilibrium condition for a single cell, which reveals a fundamental trade-off between internal feedback and external influence.

The equilibrium condition $\boldsymbol{y}^* = \tilde{\boldsymbol{D}}^{-1}\boldsymbol{B}\boldsymbol{s}(\boldsymbol{y}^*)$ can be written for a single cell C_k as:

$$y_k^* = \frac{1}{d_{C_k}} \sum_{l=1}^{M} b_{kl} s(y_l^*) = \frac{b_{kk}}{d_{C_k}} s(y_k^*) + \sum_{l \neq k} \frac{b_{kl}}{d_{C_k}} s(y_l^*).$$

This expression motivates us to define two key quantities for each cell C_k:

- The *internal influence ratio*, $\mu_k = b_{kk}/d_{C_k}$, which is the fraction of a cell's connections that are internal to itself.
- The *external influence*,

$$m_k(\boldsymbol{y}_{-k}) = \frac{1}{d_{C_k} - b_{kk}} \sum_{l \neq k} b_{kl} s(y_l),$$

  where $\boldsymbol{y}_{-k}$ is the vector of state of cells other than C_k. Thus, $m_k(\boldsymbol{y}_{-k})$ represents the weighted average of signals received from all other cells. Note that $d_{C_k} - b_{kk} = \sum_{l \neq k} b_{kl}$.

With these definitions, the equilibrium condition for cell C_k can be rewritten as a balance equation:

$$y_k^* = \mu_k s(y_k^*) + (1 - \mu_k) m_k(\boldsymbol{y}_{-k}^*). \tag{9}$$

For a fixed external influence m_k, finding the equilibrium y_k^* is equivalent to finding a fixed point of the one-dimensional function $g_k(y_k) = \mu_k s(y_k) + (1 - \mu_k)m_k$. The following lemma provides the condition for this fixed point to be unique.

Lemma 2. *Let $\mu \in [0, 1)$ and $m \in [-1, 1]$. The function $g_m(x) = \mu s(x) + (1 - \mu)m$ has a unique fixed point in $[-1, 1]$ for every $m \in [-1, 1]$ if and only if the function $h(x) = \mu s(x) - x$ is strictly decreasing on $[-1, 1]$.*

Proof. A fixed point x^* satisfies $x^* = \mu s(x^*) + (1 - \mu)m$. Define $f(x) = x - \mu s(x)$, so the condition is $f(x^*) = C$, where $C = (1 - \mu)m$. As m varies in $[-1, 1]$, C varies in the interval $I = [-(1 - \mu), 1 - \mu]$. The lemma is equivalent to stating: the equation $f(x) = C$ has a unique solution $x \in [-1, 1]$ for every $C \in I$ if and only if $f(x)$ is strictly increasing on $[-1, 1]$ (since $f = -h$).

($\Leftarrow$) Assume $f(x)$ is strictly increasing. Then f is injective, guaranteeing at most one solution for any C. We evaluate the endpoints: $f(-1) = -1 - \mu s(-1) \leq -1 + \mu = -(1 - \mu)$ and $f(1) = 1 - \mu s(1) \geq 1 - \mu$. Since f is continuous, by the Intermediate Value Theorem, the range $f([-1, 1])$ contains $[f(-1), f(1)]$, which includes I. Thus, for every $C \in I$, a solution exists. Existence plus injectivity yields uniqueness.

($\Rightarrow$) Assume that for every $m \in [-1, 1]$, g has a unique fixed point. We prove by contradiction, assuming $f(x)$ is not strictly increasing. Since f is continuous, if it is not strictly increasing, it cannot be injective. Therefore, there exist $x_1 < x_2$ in $[-1, 1]$ such that $f(x_1) = f(x_2)$. Let $C_0 = f(x_1) = f(x_2)$. If $C_0 \in I = [-(1 - \mu), 1 - \mu]$, then for the value $m_0 = C_0/(1 - \mu) \in [-1, 1]$, the equation $f(x) = C_0$ has at least two solutions. Thus, there are two fixed points of $g(x)$ for m_0. This contradicts the premise that the fixed point is unique for all $m \in [-1, 1]$.

Therefore, the condition holds if and only if $f(x)$ is strictly increasing, which is equivalent to $h(x) = -f(x)$ being strictly decreasing. □

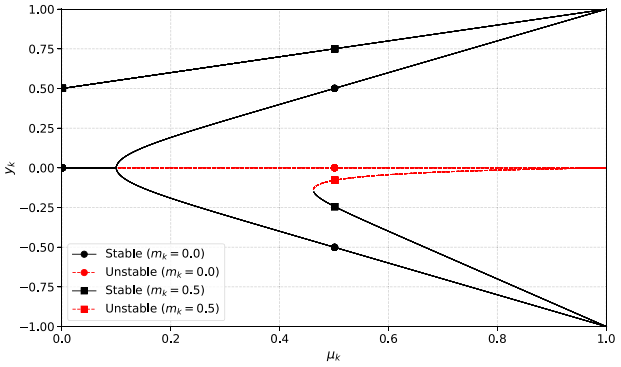

Fig. 2. Bifurcation diagram of (9) for different values of $m(\boldsymbol{y}_{-k})$ with $s(x) = \tanh(10x)$. The red dashed line represents unstable fixed points, and the black line represents stable fixed points. The markers represent the fixed points for the different values of m. For $m = 0$, there is a pitchfork bifurcation at $\mu_k = 0.1$ while for $m = 0.5$, there is a perturbed pitchfork bifurcation at $\mu_k = 0.5$.

This lemma allows us to connect the network structure (via μ_k) to the potential for multiple equilibria. A high internal influence μ_k combined with a strong nonlinearity in s can cause $h(x)$ to lose its monotonicity, leading to bifurcations. For a fixed external influence $m_k(\boldsymbol{y}_{-k})$, we can define the parameterized function $g_k(y_k; \boldsymbol{y}_{-k}) = \mu_k s(y_k) + (1 - \mu_k) m_k(\boldsymbol{y}_{-k})$ and formulate the following proposition.

Proposition 5. *Let $\mathcal{G}$ be a graph with an EP $\pi = \{C_1, \dots, C_M\}$ and K be the minimum Lipschitz constant of s. Then, the following hold true.*

- *If $\mu_k K < 1$, then $g_k(y_k; \boldsymbol{y}_{-k})$ admits a unique fixed point for any fixed $\boldsymbol{y}_{-k} \in [-1, 1]^{M-1}$.*
- *If $\mu_k K > 1$, there exists $\boldsymbol{y}_{-k} \in [-1, 1]^{M-1}$ such that $g_k(y_k; \boldsymbol{y}_{-k})$ admits multiple fixed points in its first argument y_k.*

Proof. Let us first assume that $\mu_k K < 1$. One can verify that g_k is a contraction mapping on its first argument y_k for any fixed $\boldsymbol{y}_{-k} \in [-1, 1]^{M-1}$. Indeed, for any $y_k, \tilde{y}_k \in [-1, 1]$,

$$\left| g_k(y_k; \boldsymbol{y}_{-k}) - g_k(\tilde{y}_k; \boldsymbol{y}_{-k}) \right| = \left| \mu_k (s(y_k) - s(\tilde{y}_k)) \right| \leq \mu_k K \left| y_k - \tilde{y}_k \right| < \left| y_k - \tilde{y}_k \right|.$$

Therefore, g_k admits a unique fixed point in its first argument y_k for any $\boldsymbol{y}_{-k} \in [-1, 1]^{M-1}$.

Assume now that $\mu_k > 1/K$. Then, $1/\mu_k \leq K$ and since s is non-decreasing and with minimum Lipschitz constant K, we have $\sup_{y_a \neq y_b} (s(y_b) - s(y_a))/(y_b - y_a) = K$. This means that there exist $y_a, y_b \in [-1, 1]$ with $y_a < y_b$ such that $(s(y_b) - s(y_a))/(y_b - y_a) \geq K \geq 1/\mu_k$. Then, by rearranging,

$$\frac{s(y_b) - s(y_a)}{y_b - y_a} \geq \frac{1}{\mu_k} \Leftrightarrow \mu_k s(y_b) - y_b \geq \mu_k s(y_a) - y_a \Leftrightarrow h(y_b) \geq h(y_a),$$

where $h(y) = \mu_k s(y) - y$. Thus, since $m_k(\boldsymbol{y}_{-k}) \in [-1, 1]$, if such $y_a < y_b$ exist, we have $h(y_b) \geq h(y_a)$ implying that $h(y_k)$ is not strictly decreasing. Then, from Lemma 2, g_k admits multiple fixed points in its first argument y_k for some values of $\boldsymbol{y}_{-k} \in [-1, 1]^{M-1}$. □

Remark 5. Proposition 5 exhibits that cells with high internal connectivity (large μ_k) are more susceptible to self-organizing into multiple distinct states, driven by the nonlinearity of s. This provides a direct link between the graph's structure and the complexity of its equilibrium landscape, as illustrated in Fig. 2.

6. Stability of local agreement equilibria

While the existence of a CSE is guaranteed, its stability is not. We now derive conditions for the local exponential stability of an equilibrium $\boldsymbol{x}^* = \boldsymbol{P}\boldsymbol{y}^*$ for specific kind of perturbations. For simplicity of the presentation, we will assume that a continuously differentiable signal function s. The core of our analysis is to decompose the stability problem, leveraging the invariant manifold structure of $\mathcal{S}_\pi$. Although the local stability of any equilibria $\boldsymbol{x}^*$ can be studied by looking at the Jacobian matrix of the full system, this may not be suitable or computationally feasible for very large graphs. On the other hand, the quotient system may be low-dimensional and thus easier to handle.

6.1. Quotient stability

First, we analyze the system's response to perturbations *along* the manifold $\mathcal{S}_\pi$, where the average state of each cluster is perturbed but internal synchronization is preserved. For example, the state moves from $\boldsymbol{x}^* = \boldsymbol{P}\boldsymbol{y}^*$ to a perturbed state $\boldsymbol{x} = \boldsymbol{P}(\boldsymbol{y}^* + \varepsilon \boldsymbol{y})$.

The stability against these perturbations is entirely determined by the dynamics of $\boldsymbol{y}^*$ as an equilibrium of the M-dimensional quotient dynamics (8). Consequently, for the cluster configuration to be stable, the equilibrium $\boldsymbol{y}^*$ must be a stable equilibrium of the quotient dynamics. To assess this, we linearize the system around the equilibrium $\boldsymbol{y}^*$, which yields the *quotient Jacobian matrix*:

$$\boldsymbol{J}_{\text{quot}}(\boldsymbol{y}^*) := \tilde{\boldsymbol{D}}^{-1}\boldsymbol{B}\boldsymbol{s}'(\boldsymbol{y}^*) - \boldsymbol{I}_M, \tag{10}$$

where $\boldsymbol{s}'(\boldsymbol{y}^*) = \text{diag}(s'(y_1^*), \dots, s'(y_M^*))$.

We establish the relationship between the quotient and full system spectra via the following lemma.

Lemma 3 (*Spectral Inclusion*)**.** *Let $\boldsymbol{x}^* = \boldsymbol{P}\boldsymbol{y}^*$ be a CSE. The spectrum of the quotient Jacobian $\boldsymbol{J}_{\text{quot}}(\boldsymbol{y}^*)$ is a subset of the spectrum of the full Jacobian $\boldsymbol{J}(\boldsymbol{x}^*)$. Specifically, for every eigenpair $(\lambda, \boldsymbol{v})$ of $\boldsymbol{J}_{\text{quot}}(\boldsymbol{y}^*)$, $(\lambda, \boldsymbol{P}\boldsymbol{v})$ is an eigenpair of $\boldsymbol{J}(\boldsymbol{x}^*)$.*

Proof. We show that the Jacobian matrices satisfy the intertwining relation $\boldsymbol{J}(\boldsymbol{x}^*)\boldsymbol{P} = \boldsymbol{P}\boldsymbol{J}_{\text{quot}}(\boldsymbol{y}^*)$. Recall the definitions $\boldsymbol{J}(\boldsymbol{x}^*) = \boldsymbol{D}^{-1}\boldsymbol{A}\boldsymbol{s}'(\boldsymbol{x}^*) - \boldsymbol{I}_N$ and $\boldsymbol{J}_{\text{quot}}(\boldsymbol{y}^*) = \tilde{\boldsymbol{D}}^{-1}\boldsymbol{B}\boldsymbol{s}'(\boldsymbol{y}^*) - \boldsymbol{I}_M$.

Since $\boldsymbol{x}^* \in \mathcal{S}_\pi$, we have $\boldsymbol{s}'(\boldsymbol{x}^*)\boldsymbol{P} = \boldsymbol{P}\boldsymbol{s}'(\boldsymbol{y}^*)$. Using this and the identities from Lemma 1:

$$\begin{aligned}
\boldsymbol{J}(\boldsymbol{x}^*)\boldsymbol{P} &= (\boldsymbol{D}^{-1}\boldsymbol{A}\boldsymbol{s}'(\boldsymbol{x}^*) - \boldsymbol{I}_N)\boldsymbol{P} = \boldsymbol{D}^{-1}\boldsymbol{A}\boldsymbol{P}\boldsymbol{s}'(\boldsymbol{y}^*) - \boldsymbol{P} \\
&= \boldsymbol{D}^{-1}\boldsymbol{P}\boldsymbol{B}\boldsymbol{s}'(\boldsymbol{y}^*) - \boldsymbol{P} \quad (\text{using } \boldsymbol{A}\boldsymbol{P} = \boldsymbol{P}\boldsymbol{B}) \\
&= \boldsymbol{P}\tilde{\boldsymbol{D}}^{-1}\boldsymbol{B}\boldsymbol{s}'(\boldsymbol{y}^*) - \boldsymbol{P} \quad (\text{using } \boldsymbol{D}^{-1}\boldsymbol{P} = \boldsymbol{P}\tilde{\boldsymbol{D}}^{-1}) \\
&= \boldsymbol{P}\left(\tilde{\boldsymbol{D}}^{-1}\boldsymbol{B}\boldsymbol{s}'(\boldsymbol{y}^*) - \boldsymbol{I}_M\right) \\
&= \boldsymbol{P}\boldsymbol{J}_{\text{quot}}(\boldsymbol{y}^*).
\end{aligned}$$

Let $(\lambda, \boldsymbol{v})$ be an eigenpair of $\boldsymbol{J}_{\text{quot}}(\boldsymbol{y}^*)$. Multiplying the relation by $\boldsymbol{v}$ from the right yields:

$$\boldsymbol{J}(\boldsymbol{x}^*)(\boldsymbol{P}\boldsymbol{v}) = \boldsymbol{P}\boldsymbol{J}_{\text{quot}}(\boldsymbol{y}^*)\boldsymbol{v} = \boldsymbol{P}(\lambda\boldsymbol{v}) = \lambda(\boldsymbol{P}\boldsymbol{v}).$$

Since $\boldsymbol{P}$ has full column rank (by definition of $\boldsymbol{P}$, see Example 1), $\boldsymbol{P}\boldsymbol{v} \neq \boldsymbol{0}$, proving that $\boldsymbol{P}\boldsymbol{v}$ is an eigenvector of $\boldsymbol{J}(\boldsymbol{x}^*)$ associated with λ. □

This inclusion allows us to formally state the necessary and sufficient condition for stability with respect to perturbations within the manifold $\mathcal{S}_\pi$.

Proposition 6 (*Quotient Stability*)**.** *Let $\boldsymbol{x}^* = \boldsymbol{P}\boldsymbol{y}^*$ be a CSE for an EP π. Assume that the signal function s is continuously differentiable in a neighborhood of each component of $\boldsymbol{y}^*$. The equilibrium $\boldsymbol{x}^*$ is exponentially stable with respect to perturbations restricted to the invariant subspace $\mathcal{S}_\pi$ if and only if the quotient Jacobian $\boldsymbol{J}_{\text{quot}}(\boldsymbol{y}^*)$ is Hurwitz.*

Proof. The dynamics restricted to the invariant subspace $\mathcal{S}_\pi$ is topologically conjugate to the linear system $\dot{\boldsymbol{z}} = \boldsymbol{J}_{\text{quot}}(\boldsymbol{y}^*)\boldsymbol{z}$ via the coordinate transformation $\boldsymbol{x} = \boldsymbol{P}\boldsymbol{z}$. Therefore, the restricted system is exponentially stable if and only if all eigenvalues of $\boldsymbol{J}_{\text{quot}}(\boldsymbol{y}^*)$ have strictly negative real parts (i.e., $\boldsymbol{J}_{\text{quot}}(\boldsymbol{y}^*)$ is Hurwitz). This is a direct consequence of the linearization principle (see [28]). □

6.2. Transversal stability

Second, we must analyze perturbations *transversal* to the manifold $\mathcal{S}_\pi$, which break the synchronization within one or more cells. For example, two agents i, j within the same cell C_k are perturbed from their common state y_k^* such that their new states are no longer identical. Transversal stability requires that the system dynamics actively suppress such internal disagreements, forcing the states of agents within any given cell to re-synchronize. If this condition is not met, a cell could "break apart" and lose its coherence, even if the cell's average state remains stable according to the quotient dynamics. Those properties fall into two categories:

- *Internal Cohesion:* Each cell C_k must possess internal dynamics that are inherently stable.
- *Inter-Cell Coupling:* Disagreements are coupled across cells. A perturbation in cell C_j can propagate and destabilize cell C_k.

To emphasize this decomposition, let us consider a small perturbation $\boldsymbol{\delta}$ around $\boldsymbol{x}^*$. Its linearized dynamics is $\dot{\boldsymbol{\delta}} = \boldsymbol{J}(\boldsymbol{x}^*)\boldsymbol{\delta}$. We focus on the block of equations corresponding to the agents in a cell C_k. The perturbation sub-vector $\boldsymbol{\delta}_k$ evolves according to:

$$\dot{\boldsymbol{\delta}}_k = \left(\boldsymbol{J}(\boldsymbol{x}^*)\boldsymbol{\delta}\right)_k = \sum_{j=1}^{M} \boldsymbol{J}_{kj}\boldsymbol{\delta}_j = \boldsymbol{J}_{kk}\boldsymbol{\delta}_k + \sum_{j\neq k} \boldsymbol{J}_{kj}\boldsymbol{\delta}_j,$$

where $\boldsymbol{J}_{kj}$ is the (k, j)-th block of the Jacobian $\boldsymbol{J}(\boldsymbol{x}^*)$. From the definition of $\boldsymbol{J}(\boldsymbol{x}^*)$, these blocks are:

$$\boldsymbol{J}_{kk} = \frac{s'(y_k^*)}{d_{C_k}}\boldsymbol{A}_k - \boldsymbol{I}_{N_k} \text{ and } \boldsymbol{J}_{kj} = \frac{s'(y_j^*)}{d_{C_k}}\boldsymbol{A}_{kj} \quad \text{for } k \neq j.$$

Moreover, the disagreement vector dynamics of in cell C_k is given by $\boldsymbol{e}_k = \Pi_k^{\perp}\boldsymbol{\delta}_k$ and is found by applying the projection operator $\Pi_k^{\perp} := \boldsymbol{I}_{N_k} - \frac{1}{N_k}\mathbf{1}_{N_k}\mathbf{1}_{N_k}^{\top}$ to the dynamics of $\boldsymbol{\delta}_k$:

$$\dot{\boldsymbol{e}}_k = (\dot{\Pi_k^{\perp}}\boldsymbol{\delta}_k) = \Pi_k^{\perp}\dot{\boldsymbol{\delta}}_k = \underbrace{\Pi_k^{\perp}\left[\frac{s'(y_k^*)}{d_{C_k}}\boldsymbol{A}_k - \boldsymbol{I}_{N_k}\right]\boldsymbol{\delta}_k}_{\text{Internal}} + \underbrace{\sum_{j\neq k}\Pi_k^{\perp}\frac{s'(y_j^*)}{d_{C_k}}\boldsymbol{A}_{kj}\boldsymbol{\delta}_j}_{\text{Inter-Cell}}. \tag{11}$$

Internal cohesion stability

In this part, we will focus only on perturbations inside a specific cell C_k for some $k \in \{1, \dots, M\}$. This means that for all $j \neq k$, $\boldsymbol{\delta}_j = \mathbf{0}$. To measure the internal cohesion, we define the *internal error decay rate* of the cell k,

$$\alpha_k(y_k^*) := 1 - \frac{s'(y_k^*)}{d_{C_k}}\lambda_{N_k-1}(\boldsymbol{A}_k). \tag{12}$$

where $\lambda_{N_k-1}(\boldsymbol{A}_k)$ is the second largest eigenvalue of the induced subgraph matrix $\boldsymbol{A}_k$. One has the following proposition:

Proposition 7. *Let $\boldsymbol{x}^* = \boldsymbol{P}\boldsymbol{y}^*$ be a CSE resulting from a connected EP π. Then, the equilibrium $\boldsymbol{x}^*$ is exponentially locally stable for any perturbation along $\mathbb{1}_{C_k}$ (i.e., inside the cell) if and only if $\alpha_k(y_k^*) > 0$.*

Proof. Considering perturbation only inside the cell (i.e., along $\mathbb{1}_{C_k}$) of a CSE is equivalent to studying the error dynamics (11) without the inter-cell part since $\boldsymbol{\delta}_j = \mathbf{0}$ for all $j \neq k$. Let us focus on the internal part of (11).

The EP structure implies that the adjacency matrix of the induced subgraph of C_k, $\boldsymbol{A}_k$, has a constant row sum b_{kk}. This means $\boldsymbol{A}_k\mathbf{1}_{N_k} = b_{kk}\mathbf{1}_{N_k}$, so $\boldsymbol{A}_k$ and the projector $\Pi_k^{\perp}$ commute. Therefore:

$$\Pi_k^{\perp}\boldsymbol{J}_{kk}\boldsymbol{\delta}_k = \Pi_k^{\perp}\left(\frac{s'(y_k^*)}{d_{C_k}}\boldsymbol{A}_k - \boldsymbol{I}_{N_k}\right)\boldsymbol{\delta}_k = \left(\frac{s'(y_k^*)}{d_{C_k}}\boldsymbol{A}_k - \boldsymbol{I}_{N_k}\right)\Pi_k^{\perp}\boldsymbol{\delta}_k = \left(\frac{s'(y_k^*)}{d_{C_k}}\boldsymbol{A}_k - \boldsymbol{I}_{N_k}\right)\boldsymbol{e}_k.$$

Thus, the internal error dynamics of cell k around $\boldsymbol{x}^*$ is given by

$$\dot{\boldsymbol{e}}_k = \left(\frac{s'(y_k^*)}{d_{C_k}}\boldsymbol{A}_k - \boldsymbol{I}_{N_k}\right)\boldsymbol{e}_k.$$

Since this system is linear, the stability is determined by the eigenvalues of the matrix $\boldsymbol{M}_k = s'(y_k^*)\boldsymbol{A}_k/d_{C_k} - \boldsymbol{I}_{N_k}$ restricted to the subspace $\mathbf{1}_{N_k}^{\perp}$ (since $\boldsymbol{e}_k \perp \mathbf{1}_{N_k}$). The eigenvalues of $\boldsymbol{A}_k$ are $\lambda_1 \leq \cdots \leq \lambda_{N_k}$. By Perron–Frobenius Theorem (e.g., see [29]) since the graph induced by $\boldsymbol{A}_k$ is connected, its largest eigenvalue λ_{N_k} has multiplicity one and corresponds to the eigenvector $\mathbf{1}_{N_k}$ and is then irrelevant for $\boldsymbol{e}_k$. The eigenvalues of $\boldsymbol{M}_k$ governing the disagreement are $s'(y_k^*)\lambda_i(\boldsymbol{A}_k)/d_{C_k} - 1$ for $i < N_k$. The largest real part among these is determined by λ_{N_k-1} with the maximum eigenvalue being $s'(y_k^*)\lambda_{N_k-1}(\boldsymbol{A}_k)/d_{C_k} - 1 = -\alpha_k(y_k^*)$. Thus, by the linearization principle, the system is stable if and only if $\alpha_k(y_k^*) > 0$. □

Inter-cell coupling stability

When cells are interconnected, disagreements can propagate. We model this via a comparison system involving the norms of the errors. Define the *coupling gain matrix* $\boldsymbol{G} \in \mathbb{R}^{M\times M}$:

$$G_{kj} = \begin{cases} -\alpha_k(y_k^*) & \text{if } k = j \\ \dfrac{s'(y_j^*)}{d_{C_k}}\sqrt{b_{kj}b_{jk}} & \text{if } k \neq j. \end{cases} \tag{13}$$

Remark 6. Note that if a cell C_k has $N_k = 1$, it is trivially connected, and the Transversal Stability condition (12) does not apply to that cell.

Proposition 8 (*Transversal Stability*)**.** *Let $\boldsymbol{x}^* = \boldsymbol{P}\boldsymbol{y}^*$ be a CSE resulting from a connected EP π. Assume that for all cells with $N_k \geq 2$, $\alpha_k(y_k^*) > 0$. If the coupling gain matrix $\boldsymbol{G}$ defined in (13) is Hurwitz, then the transversal dynamics is locally exponentially stable (i.e., $\boldsymbol{e}(t) \to \mathbf{0}$ exponentially).*

Proof. Since the destabilization part emerging from the internal cohesion has been characterized in Proposition 7, let us focus on the inter-cell perturbation.

For the external influence, we decompose the perturbation $\boldsymbol{\delta}_j$ from another cell C_j into its average component and its disagreement component: $\boldsymbol{\delta}_j = \bar{\delta}_j\mathbf{1}_{N_j} + \boldsymbol{e}_j$. As before $\boldsymbol{A}_{kj}$ (the $N_k \times N_j$ block of $\boldsymbol{A}$) has a constant row sum b_{kj}, thus, $\boldsymbol{A}_{kj}\mathbf{1}_{N_j} = b_{kj}\mathbf{1}_{N_k}$. The projection of the influence from the average part of $\boldsymbol{\delta}_j$ is:

$$\Pi_k^{\perp}\boldsymbol{A}_{kj}(\bar{\delta}_j\mathbf{1}_{N_j}) = \bar{\delta}_j\Pi_k^{\perp}(\boldsymbol{A}_{kj}\mathbf{1}_{N_j}) = \bar{\delta}_j\Pi_k^{\perp}(b_{kj}\mathbf{1}_{N_k}) = \mathbf{0}.$$

The average perturbation from other cells does not affect the internal disagreement dynamics. The only influence comes from the disagreement vectors $\boldsymbol{e}_j$:

$$\Pi_k^{\perp} \boldsymbol{J}_{kj} \boldsymbol{\delta}_j = \frac{s'(y_j^*)}{d_{C_k}} \Pi_k^{\perp} \boldsymbol{A}_{kj} (\bar{\delta}_j \mathbf{1}_{N_j} + \boldsymbol{e}_j) = \frac{s'(y_j^*)}{d_{C_k}} \Pi_k^{\perp} \boldsymbol{A}_{kj} \boldsymbol{e}_j.$$

Combining these terms and defining the external influence as $\boldsymbol{u}_k = \sum_{j \neq k} s'(y_j^*) \boldsymbol{A}_{kj} \boldsymbol{e}_j$, we get the equation for the transversal dynamics:

$$\dot{\boldsymbol{e}}_k = \left(\frac{s'(y_k^*)}{d_{C_k}} \boldsymbol{A}_k - \boldsymbol{I}_{N_k} \right) \boldsymbol{e}_k + \frac{1}{d_{C_k}} \Pi_k^{\perp} \boldsymbol{u}_k.$$

For each subsystem k, we define the degree-weighted Lyapunov function: $V_k(\boldsymbol{e}_k) = d_{C_k} \|\boldsymbol{e}_k\|^2/2$. Its time derivative along the trajectories of the disagreement dynamics is:

$$\dot{V}_k(\boldsymbol{e}_k) = d_{C_k} \boldsymbol{e}_k^{\top} \dot{\boldsymbol{e}}_k = \boldsymbol{e}_k^{\top} \left(s'(y_k^*) \boldsymbol{A}_k - d_{C_k} \boldsymbol{I}_{N_k} \right) \boldsymbol{e}_k + \boldsymbol{e}_k^{\top} \Pi_k^{\perp} \boldsymbol{u}_k.$$

For the first term, using the Courant–Fischer theorem, since $\boldsymbol{e}_k \perp \mathbf{1}_{N_k}$ it yields $\boldsymbol{e}_k^{\top} \boldsymbol{A}_k \boldsymbol{e}_k \leq \lambda_{N_k-1}(\boldsymbol{A}_k) \|\boldsymbol{e}_k\|^2$. Thus, one has

$$\begin{aligned} \boldsymbol{e}_k^{\top} (s'(y_k^*) \boldsymbol{A}_k - d_{C_k} \boldsymbol{I}_{N_k}) \boldsymbol{e}_k &\leq (s'(y_k^*) \lambda_{N_k-1}(\boldsymbol{A}_k) - d_{C_k}) \|\boldsymbol{e}_k\|^2 \\ &= -\left[d_{C_k} - s'(y_k^*) \lambda_{N_k-1}(\boldsymbol{A}_k) \right] \|\boldsymbol{e}_k\|^2 = -d_{C_k} \alpha_k(y_k^*) \|\boldsymbol{e}_k\|^2. \end{aligned}$$

For the second term, Cauchy–Schwarz gives $\boldsymbol{e}_k^{\top} \boldsymbol{u}_k \leq \|\boldsymbol{e}_k\| \cdot \|\boldsymbol{u}_k\|$. We bound the input norm $\|\boldsymbol{u}_k\|$ by

$$\|\boldsymbol{u}_k\| = \left\| \sum_{j \neq k} s'(y_j^*) \boldsymbol{A}_{kj} \boldsymbol{e}_j \right\| \leq \sum_{j \neq k} s'(y_j^*) \|\boldsymbol{A}_{kj}\|_2 \cdot \|\boldsymbol{e}_j\|.$$

Using the spectral norm bound for adjacency matrix (e.g., see [30]), $\|\boldsymbol{A}_{kj}\|_2 \leq \sqrt{b_{kj} b_{jk}}$, we have:

$$\|\boldsymbol{u}_k\| \leq \sum_{j \neq k} s'(y_j^*) \sqrt{b_{kj} b_{jk}} \|\boldsymbol{e}_j\|.$$

Thus, this yields the differential inequality:

$$\dot{V}_k(\boldsymbol{e}_k) \leq -d_{C_k} \alpha_k(y_k^*) \|\boldsymbol{e}_k\|^2 + \|\boldsymbol{e}_k\| \cdot \sum_{j \neq k} s'(y_j^*) \sqrt{b_{kj} b_{jk}} \|\boldsymbol{e}_j\|. \tag{14}$$

Let $z_k(t) = \|\boldsymbol{e}_k(t)\|$. Substituting z_k in (14) (and dividing by z_k for $z_k \neq 0$) gives a system of linear differential inequalities for the vector of norms $\boldsymbol{z}$:

$$\dot{z}_k \leq -\alpha_k(y_k^*) z_k + \sum_{j \neq k} \frac{s'(y_j^*)}{d_{C_k}} \sqrt{b_{kj} b_{jk}} z_j,$$

which can be written as $\dot{\boldsymbol{z}} \leq \boldsymbol{G}\boldsymbol{z}$. By the Comparison Lemma, if the linear system $\dot{\boldsymbol{\eta}} = \boldsymbol{G}\boldsymbol{\eta}$ is exponentially stable (i.e., if $\boldsymbol{G}$ is Hurwitz), then $\boldsymbol{z}(t)$ converges exponentially to zero. This establishes the local exponential stability of the synchronization manifold S_π. □

Remark 7 (*Connected EP Assumption*)**.** The assumption that the EP π is connected ensures that each induced subgraph $\mathcal{G}_k$ is connected. If the connectivity assumption on the partition is dropped, a cell C_k with $N_k \geq 2$ might have $b_{kk} = 0$ (no internal edges). In this scenario, $\boldsymbol{D}_k = \mathbf{0}$ and $\boldsymbol{L}_k = -\boldsymbol{A}_k$. The stability matrix for transversal modes becomes $\boldsymbol{M}_k = s'(y_k^*) \boldsymbol{A}_k - \boldsymbol{I}_{N_k}$. Stability then requires $s'(y_k^*) \lambda_j(\boldsymbol{A}_k) < 1$ for all eigenvalues $\lambda_j(\boldsymbol{A}_k)$ of $\boldsymbol{A}_k$ corresponding to transversal modes.

6.3. Main stability theorem

We combine the analyses of the quotient and transversal dynamics to provide sufficient conditions for the full local stability of the equilibrium.

Theorem 1. *Let $\boldsymbol{x}^* = \boldsymbol{P}\boldsymbol{y}^*$ be a CSE resulting from a connected EP π. Assume the signal function s is continuously differentiable. If the following conditions hold:*

(i) Quotient Stability: The quotient Jacobian matrix $\boldsymbol{J}_{\text{quot}}(\boldsymbol{y}^*)$ defined in (10) is Hurwitz.

(ii) Transversal Stability: For every cell C_k with $N_k \geq 2$, the internal decay rate is positive ($\alpha_k(y_k^*) > 0$) and the coupling gain matrix $\boldsymbol{G}$ defined in (13) is Hurwitz.

Then, the equilibrium $\boldsymbol{x}^*$ is locally exponentially stable.

Conversely, if $\boldsymbol{x}^*$ is locally exponentially stable, then $\boldsymbol{J}_{\text{quot}}(\boldsymbol{y}^*)$ is Hurwitz and $\alpha_k(y_k^*) > 0$ for all k.

Proof. The eigenvalues of the full Jacobian $\boldsymbol{J}(\boldsymbol{x}^*)$ determine local stability. By Lemma 3, the set of eigenvalues of $\boldsymbol{J}_{\text{quot}}(\boldsymbol{y}^*)$ is a subset of the eigenvalues of $\boldsymbol{J}(\boldsymbol{x}^*)$. (i) ensures that these M eigenvalues have strictly negative real parts.

The remaining $N - M$ eigenvalues govern the dynamics of the disagreement subspace (transversal dynamics). (ii) ensures, via Proposition 8, that the transversal dynamics is exponentially stable. Since both invariant subspaces are stable, the full system is locally exponentially stable.

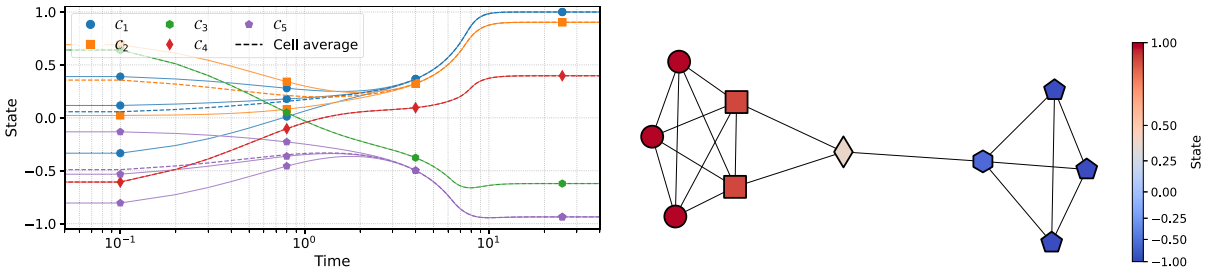

(a) State trajectories over time (log scale). (b) Asymptotic network state configuration.

Fig. 3. Numerical verification of the stability of a CSE applied to Opinion Dynamics. The simulation uses the graph topology from Fig. 1(a) and a saturation interaction function $s(x) = \min(1, \max(-1, Kx))$ with $K = 1.2$. The state $x_i \in [-1, 1]$ represents the normalized opinion of agent i on a topic (where -1 and $+1$ denote extreme opposing views). The saturation function models the bounded influence agents have on their neighbors via nonlinear interaction. **(a)** Time evolution of opinions. The **solid lines** represent individual agent opinions. Multiple curves of the same color correspond to different agents in the same cluster starting with random initial views. The **dashed lines** represent the average opinion of each cluster. **(b)** The steady-state of opinions ($t = 30$). Node shapes indicate membership in specific social clusters (cells $C_1, \dots, C_5$), while the color gradient represents the final opinion value. The uniform color within each group confirms that agents within the same social cluster have reached a local consensus (polarization). The plot illustrates the formation of "echo chambers": agents rapidly align with their immediate cluster (transversal stability), followed by the slower settling of the clusters' collective opinions (quotient stability). The simulation code is available at [31].

Conversely, if $\boldsymbol{J}(\boldsymbol{x}^*)$ is Hurwitz, then its subset of eigenvalues corresponding to $\boldsymbol{J}_{\text{quot}}$ must be stable (Proposition 6), and the diagonal blocks corresponding to internal modes must be stable (Proposition 7), implying $\alpha_k(y_k^*) > 0$. □

Fig. 3 provides a numerical illustration of convergence to a stable CSE on the graph from Fig. 1. The top panel shows the final polarized state, where agents within each cell (identified by shape) have reached a common value (uniform color). The bottom panel displays the system's trajectories, revealing a clear two-stage dynamic. First, individual agent states (thin solid lines) rapidly contract onto their respective cell averages (dashed lines), demonstrating the system's *transversal stability*. Subsequently, these cell averages converge more slowly to their final equilibrium values, governed by the stable quotient dynamics, thereby confirming *quotient stability*. The simulation provides a concrete validation of the stability decomposition established in Theorem 1.

Remark 8 (*Relaxation of Smoothness of s*)**.** The previous Propositions and Theorem assume that the signal function s is continuously differentiable near the equilibrium $\boldsymbol{x}^*$. While this facilitates a tractable proof using standard linearization, the result can theoretically be extended to non-smooth, Lipschitz continuous signals (e.g., piecewise linear functions) using non-smooth analysis tools such as Clarke generalized Jacobian (e.g., see [32, Section 1.3]). In that framework, the scalar derivative $s'(y_k^*)$ in conditions (10) and (12) would be replaced by elements of the generalized gradient set $\partial s(y_k^*)$. Stability would then require that the quotient and transversal conditions hold for all values within this set.

Remark 9 (*Stability in Directed Graphs*)**.** While the structural reduction holds for directed graphs, the stability conditions in Propositions 7, 8 and in Theorem 1 require modification due to the asymmetry of $\boldsymbol{A}$.

For Proposition 7, the proof relies on the derivative of $\|\boldsymbol{e}_k\|^2$, which generates the quadratic form $\boldsymbol{e}_k^\top \boldsymbol{A}_k \boldsymbol{e}_k$. For directed graphs, this term is governed by the symmetric part of the matrix, $\boldsymbol{A}_k^{\text{sym}} = (\boldsymbol{A}_k + \boldsymbol{A}_k^\top)/2$. Consequently, for a directed graph, the internal decay rate α_k in (12) must be defined using the eigenvalues of $\boldsymbol{A}_k^{\text{sym}}$ rather than $\boldsymbol{A}_k$:

$$\alpha_k^{\text{sym}}(y_k^*) := 1 - \frac{s'(y_k^*)}{d_{C_k}} \lambda_{N_k-1}(\boldsymbol{A}_k^{\text{sym}}).$$

Furthermore, in the proof of Proposition 8, the bound on the cross-coupling term $\|\boldsymbol{A}_{kj}\|_2$ in (13) no longer simplifies to $\sqrt{b_{kj} b_{jk}}$. From [30], it is instead bounded by $\sqrt{b_{kj} c_{kj}}$, where c_{kj} is the maximum column sum of the block $\boldsymbol{A}_{kj}$ (representing the maximum number of incoming edges from cell C_k to a single agent in C_j).

Remark 10 (*Robustness to Approximate Partitions*)**.** While Definition 4 requires exact algebraic symmetry, real-world networks often exhibit only approximate structural regularity. Following recent developments in spectral graph theory and synchronization from [19], one can define a *quasi-equitable partition* by introducing a deviation matrix $\boldsymbol{E} = \boldsymbol{AP} - \boldsymbol{PB}$, where $\|\boldsymbol{E}\|$ represents the structural error (e.g., variance in row sums). In our context, this structural mismatch acts as a perturbation to the quotient dynamics. Specifically, the invariance condition $\dot{\boldsymbol{x}} = \boldsymbol{P}\dot{\boldsymbol{y}}$ is violated by a term proportional to $\boldsymbol{E}s(\boldsymbol{x})$. However, since the signal function s is bounded on the invariant set $\mathcal{X}$ (see Remark 1), this structural perturbation is uniformly bounded. Consequently, if the nominal quotient system (Theorem 1) is exponentially stable, standard robust stability arguments (e.g., Input-to-State Stability) imply that the trajectories of the approximate system will converge to a bounded neighborhood of the synchronization manifold $\mathcal{S}_\pi$, the size of which is proportional to the structural error $\|\boldsymbol{E}\|$.

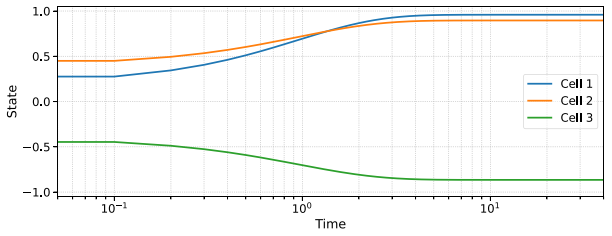

(a) **Quotient graph:** State trajectories over time (log scale).

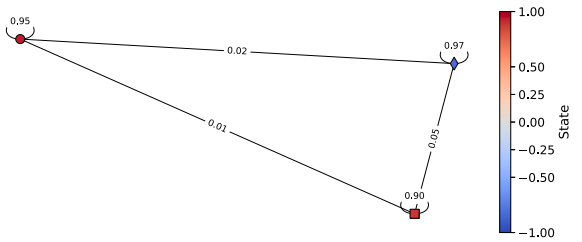

(b) **Quotient graph:** Asymptotic network state configuration.

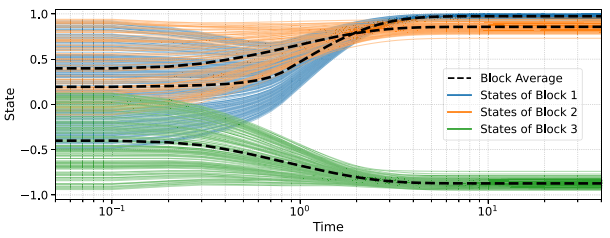

(c) **Stochastic Block Model:** State trajectories over time (log scale).

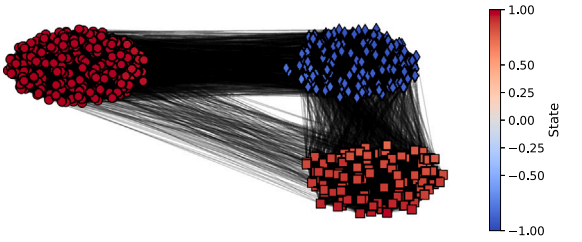

(d) **Stochastic Block Model:** Asymptotic network state configuration.

Fig. 4. Robustness of cluster synchronization on an approximate equitable partition. Comparison between an ideal quotient system (Exact EP) and a large random graph, that is an Approximate EP, graph generated through a Stochastic Block Model (SBM). The SBM consists of $N = 500$ agents divided into 3 blocks of sizes $N_1 = 250$, $N_2 = 100$, and $N_3 = 150$. The connection probabilities match the weights of the quotient graph shown in **(b)**. The interaction function is $s(x) = \min(1, \max(-1, 10x))$. **(a)** Ideal trajectories of the quotient system ($\dot{\boldsymbol{y}} = \tilde{\boldsymbol{D}}^{-1}\boldsymbol{B}s(\boldsymbol{y}) - \boldsymbol{y}$). **(b)** Topology of the quotient graph. The three nodes (circle, square, diamond) represent the cells; edge labels indicate the connection degree between blocks. **(c)** Trajectories of the SBM system. The **solid colored lines** are individual agents; the **black dashed lines** are the block averages. Note that the block averages in (c) closely match the ideal trajectories in (a). Unlike the exact case, agents do not converge to a single value but remain confined within a bounded "tube" around the average, confirming the practical stability predicted in Remark 10. **(d)** Topology of the SBM graph. The three blocks are visually distinct, with dense internal connections and sparse links between them. The simulation code is available at [31].

Fig. 4 illustrates this phenomenon. We construct a quotient graph (Fig. 4(b)) representing the ideal topology of a Stochastic Block Model (SBM) with 3 blocks (see [33]). Fig. 4(a) shows the ideal synchronization dynamics on this quotient manifold. We then simulate the full system on the SBM graph (Fig. 4(d)). Although the SBM partition is not exactly equitable by construction, Fig. 4(c) shows that the average state of each block (black dashed lines) closely tracks the trajectory of the ideal quotient system. Individual agents do not perfectly synchronize but remain trapped in a small neighborhood around the block average, confirming the bounded error dynamics predicted by the structural perturbation analysis.

Remark 11 (*Control Design and Generative Models*)**.** The theoretical framework developed here provides a constructive method for network design. To enforce a desired clustering configuration π, one can modify a given graph $\mathcal{G}$ to satisfy the conditions of Theorem 1 via a two-step process:

(i) *Regularizing:* Replace the edge weights between any two cells C_k and C_l with their average connectivity

$$b_{kl} = \frac{1}{|C_k|} \sum_{i \in C_k} \sum_{j \in C_l} a_{ij}.$$

This operation, similar to the construction of Stochastic Block Models in [19], ensures that the partition becomes exactly equitable ($\boldsymbol{AP} = \boldsymbol{PB}$).

(ii) *Stabilization:* Adjust the self-coupling weights b_{kk} to ensure the internal decay rate $\alpha_k(y_k^*) > 0$ (Proposition 7) and the quotient stability (Proposition 6).

This highlights that while exact EPs may be rare in random graphs, they represent the expected structure of community-based generative models and are naturally achievable in engineered multi-agent systems.

7. Conclusion and perspectives

This work has established a fundamental link between network topology and emergent patterns of local synchronization in multi-agent systems with perception-based dynamics. We have proven that perfect intra-cluster synchronized equilibria are structurally supported by the presence of an equitable partition in the graph. The analytical insight is that the cell-synchronized manifold is forward invariant, allowing the N-dimensional system to be described by a lower M-dimensional quotient model. This reduction was instrumental in deriving necessary and sufficient conditions for the stability of such local synchronization according to specific

types of perturbations (in the quotient system or internal to the cell) and a sufficient condition for the local exponential stability against all types of perturbation. Future work will focus on the characterization of equilibria when the graph is approximately an equitable partition with a small M.

CRediT authorship contribution statement

Anthony Couthures: Writing – original draft, Software, Methodology, Investigation, Formal analysis, Conceptualization. **Vineeth Satheeskumar Varma:** Writing – review & editing, Validation, Conceptualization. **Samson Lasaulce:** Writing – review & editing, Validation, Supervision. **Irinel-Constantin Morărescu:** Writing – review & editing, Writing – original draft, Validation, Supervision.

Declaration of competing interest

The authors declare that they have no known competing financial interests or personal relationships that could have appeared to influence the work reported in this paper.

Data availability

No data was used for the research described in the article.

References

[1] L. Moreau, Stability of multiagent systems with time-dependent communication links, IEEE Trans. Autom. Control 50 (2) (2005) 169–182, http://dx.doi.org/10.1109/TAC.2004.841888.
[2] W. Ren, R. Beard, Consensus seeking in multiagent systems under dynamically changing interaction topologies, IEEE Trans. Autom. Control 50 (5) (2005) 655–661, http://dx.doi.org/10.1109/TAC.2005.846556.
[3] F. Bullo, S. Martinez J. Cortés, Distributed control of robotic networks, in: A Mathematical Approach to Motion Coordination Algorithms, Princeton University Press, 2009.
[4] R. Hegselmann, U. Krause, Opinion dynamics and bounded confidence models, analysis, and simulation, J. Artif. Soc. Soc. Simul. 5 (3) (2002).
[5] I.-C. Morărescu, A. Girard, Opinion dynamics with decaying confidence: Application to community detection in graphs, IEEE Trans. Autom. Control 56 (8) (2011) 1862–1873, http://dx.doi.org/10.1109/TAC.2010.2095315.
[6] C. Altafini, Consensus Problems on Networks With Antagonistic Interactions, IEEE Trans. Autom. Control 58 (4) (2013) 935–946, http://dx.doi.org/10.1109/TAC.2012.2224251.
[7] J.M. Hendrickx, A lifting approach to models of opinion dynamics with antagonisms, in: 53rd IEEE Conference on Decision and Control, IEEE, Los Angeles, CA, USA, 2014, pp. 2118–2123, http://dx.doi.org/10.1109/CDC.2014.7039711.
[8] S. Fortunato, Community detection in graphs, Phys. Rep. 486 (3) (2010) 75–174, http://dx.doi.org/10.1016/j.physrep.2009.11.002.
[9] M.E.J. Newman, M. Girvan, Finding and evaluating community structure in networks, Phys. Rev. E 69 (2) (2004) 026113, http://dx.doi.org/10.1103/PhysRevE.69.026113.
[10] R. Lambiotte, J.-C. Delvenne, M. Barahona, Random Walks, Markov Processes and the Multiscale Modular Organization of complex networks, IEEE Trans. Netw. Sci. Eng. 1 (2) (2014) 76–90, http://dx.doi.org/10.1109/TNSE.2015.2391998.
[11] N.R. Chowdhury, S. Martin I.-C. Morărescu, S. Srikant, Continuous opinions and discrete actions in social networks: A multi-agent system approach, in: 2016 IEEE 55th Conference on Decision and Control (CDC), 2016, pp. 1739–1744, http://dx.doi.org/10.1109/CDC.2016.7798516.
[12] F. Ceragioli, P. Frasca, Consensus and Disagreement: The Role of Quantized Behaviors in Opinion Dynamics, SIAM J. Control Optim. 56 (2) (2018) 1058–1080, http://dx.doi.org/10.1137/16M1083402.
[13] A. Couthures, V.S. Varma, S. Lasaulce, I.-C. Morărescu, Global synchronization of multi-agent systems with nonlinear interactions, IEEE Control. Syst. Lett. 9 (2025) 354–359, http://dx.doi.org/10.1109/LCSYS.2025.3573563.
[14] A. Bizyaeva, A. Franci, N.E. Leonard, Nonlinear Opinion Dynamics With Tunable Sensitivity, IEE Trans Autom Control. 68 (3) (2023) 1415–1430, http://dx.doi.org/10.1109/TAC.2022.3159527.
[15] A. Fontan, C. Altafini, Multiequilibria analysis for a class of collective decision-making networked systems, IEEE Trans. Control. Netw. Syst. 5 (4) (2018) 1931–1940, http://dx.doi.org/10.1109/TCNS.2017.2774014.
[16] F. Baumann, I.M. Sokolov P. Lorenz-Spreen, M. Starnini, Modeling Echo Chambers and Polarization Dynamics in Social Networks, Phys. Rev. Lett. 124 (4) (2020) 048301, http://dx.doi.org/10.1103/PhysRevLett.124.048301.
[17] M.T. Schaub, N. O'Clery, Y.N. Billeh, J.-C. Delvenne, R. Lambiotte, M. Barahona, Graph partitions and cluster synchronization in networks of oscillators, Chaos Interdiscip. J. Nonlinear Sci. 26 (9) (2016) 094821, http://dx.doi.org/10.1063/1.4961065.
[18] F. Sorrentino, L.M. Pecora, A.M. Hagerstrom, T.E. Murphy, R. Roy, Complete characterization of the stability of cluster synchronization in complex dynamical networks, Sci. Adv. 2 (4) (2016) e1501737, http://dx.doi.org/10.1126/sciadv.1501737.
[19] T. Timofeyev, A. Patania, Cluster synchronization via graph Laplacian eigenvectors, Chaos 35 (9) (2025) 093109, http://dx.doi.org/10.1063/5.0280142.
[20] M. Egerstedt, S. Martini, M. Cao, K. Camlibel, A. Bicchi, Interacting with Networks: How Does Structure Relate to Controllability in Single-Leaderconsensus networks?, IEEE Control Syst. Mag. 32 (4) (2012) 66–73, http://dx.doi.org/10.1109/MCS.2012.2195411.
[21] S. Martini, M. Egerstedt, A. Bicchi, Controllability decompositions of networked systems through quotient graphs, in: 2008 47th IEEE Conf. Decis. Control, 2008, pp. 5244–5249, http://dx.doi.org/10.1109/CDC.2008.4739213.
[22] N. O'Clery, Y. Yuan, G.-B. Stan, M. Barahona, Observability and coarse graining of consensus dynamics through the external equitable partition, Phys. Rev. E 88 (4) (2013) 042805, http://dx.doi.org/10.1103/PhysRevE.88.042805.
[23] F. Ceragioli, C. De Persis, P. Frasca, Discontinuities and hysteresis in quantized average consensus, Automatica 47 (9) (2011) 1916–1928, http://dx.doi.org/10.1016/j.automatica.2011.06.020.
[24] K. Devriendt, R. Lambiotte, Nonlinear Network Dynamics with Consensus–Dissensus Bifurcation, J. Nonlinear Sci. 31 (1) (2021) 18, http://dx.doi.org/10.1007/s00332-020-09674-1.
[25] R. Gray, A. Franci, V. Srivastava, N.E. Leonard, Multiagent Decision-Making Dynamics Inspired by Honeybees, IEEE Trans. Control. Netw. Syst. 5 (2) (2018) 793–806.

[26] A. Couthures, V. Satheeskumar Varma, S. Lasaulce, I.C. Morărescu, Analysis of an opinion dynamics model coupled with an external environmental dynamics, Chaos Solitons Fractals 189 (2024) 115719, http://dx.doi.org/10.1016/j.chaos.2024.115719.
[27] C. Godsil, G. Royle, Algebraic Graph Theory, Springer-Verlag, New-York, 2001.
[28] H.K. Khalil, Nonlinear Systems, Prentice Hall, Upper Saddle River, N. J., 2002.
[29] F. Bullo, Lectures on Network Systems, CreateSpace, North Charleston, South Carolina, 2018.
[30] J. Kwapisz, On the spectral radius of a directed graph, J. Graph Theory 23 (4) (1996) 405–411.
[31] A. Couthures, Cosa-simulator, 2025, http://dx.doi.org/10.5281/zenodo.17407391, https://github.com/AnthonyCouthures/COSA-Simulator.
[32] V. Jeyakumar, Nonsmooth vector functions and continuous optimization, no, in: Springer Optimization and Its Applications, vol. 10, Springer, New York, 2008.
[33] P.W. Holland, K.B. Laskey, S. Leinhardt, Stochastic blockmodels: First steps, Soc. Netw. 5 (2) (1983) 109–137, http://dx.doi.org/10.1016/0378-8733(83)90021-7.